analytical chemistry

Article

pubs.acs.org/ac

Flow-through Capture and *in Situ* Amplification Can Enable Rapid Detection of a Few Single Molecules of Nucleic Acids from Several Milliliters of Solution

Travis S. Schlappi,[‡] Stephanie E. McCalla,[†,‡] Nathan G. Schoepp, and Rustem F. Ismagilov*

Division of Chemistry and Chemical Engineering, California Institute of Technology, 1200 East California Boulevard, Pasadena, California 91125, United States

Supporting Information

ABSTRACT: Detecting nucleic acids (NAs) at zeptomolar concentrations (few molecules per milliliter) currently requires expensive equipment and lengthy processing times to isolate and concentrate the NAs into a volume that is amenable to amplification processes, such as PCR or LAMP. Shortening the time required to concentrate NAs and integrating this procedure with amplification on-device would be invaluable to a number of analytical fields, including environmental monitoring and clinical diagnostics. Microfluidic point-of-care (POC) devices have been designed to address these needs, but they are not able to detect NAs present in zeptomolar concentrations in short time frames because they require slow flow rates and/or they are unable to handle milliliter-scale volumes. In this paper, we theoretically and experimentally investigate a flow-through capture membrane that solves this problem by capturing NAs with high sensitivity in a short time period, followed by direct detection via amplification. Theoretical predictions guided the choice of physical parameters for a chitosan-coated nylon membrane; these predictions can also be applied generally to other capture situations with different requirements. The membrane is also compatible with *in situ* amplification, which, by eliminating an elution step enables high sensitivity and will facilitate integration of this method into sample-to-answer detection devices. We tested a wide range of combinations of sample volumes and concentrations of DNA molecules using a capture membrane with a 2 mm radius. We show that for nucleic acid detection, this approach can concentrate and detect as few as ~10 molecules of DNA with flow rates as high as 1 mL/min, handling samples as large as 50 mL. In a specific example, this method reliably concentrated and detected ~25 molecules of DNA from 50 mL of sample.

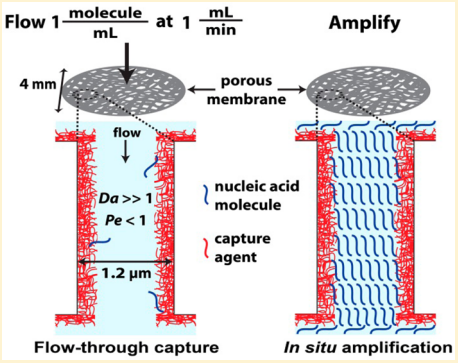

Detection of nucleic acids (NAs) at ultralow concentrations (few molecules per milliliter of sample) in short time intervals is invaluable to a number of analytical fields, including environmental monitoring and clinical diagnostics.[1−6] Pathogens in aqueous environmental samples are frequently present at or below zeptomolar concentrations (~1000 microorganisms per liter), requiring laborious filtration and concentration procedures before detection is possible.[7,8] In many clinical applications, including minimal residual diseases[9] and latent hepatitis C viral (HCV) or HIV infections, target NAs are also present at <10 molecules/mL.[10,11] Blood bank donations are typically pooled before screening, so targets may be diluted by several orders of magnitude before being screened for pathogens, generating a sample where ultrasensitive detection is critical.[12,13] Each of these examples requires the processing of large volumes (mLs) of extremely dilute samples and therefore the ability to concentrate NAs on the order of 1000X to reach PCR-suitable volumes (μLs). Additionally, the entire concentration process must be done within minutes and not rely on expensive equipment to be directly applicable to limited-resource settings (LRS) and usable at the point-of-care (POC).[14,15]

Commercial systems for the purification and concentration of nucleic acids typically involve solid phase extraction (SPE), which uses chaotropic agents to control the absorption and release of NAs on silica.[16,17] While this method is widely used, most available protocols require centralized laboratories for centrifuging samples or manipulating beads.[18] NA precipitation[19] methods are also commonly used to extract and concentrate NAs from clinical and environmental samples; however, these methods are laborious and involve the use of hazardous reagents.[20] These methods are challenging to deploy in LRS, where instrumentation is limited, or use at the POC, where diagnostics must be rapid and require minimal sample handling.[18] To address these needs, several charge-based methods have been developed, which typically include a charged polymer matrix such as chitosan or poly-L-lysine for NA capture.[21−25] In this paper, we build on such work. To increase sensitivity, these and other systems concentrate NAs and then either elute before amplification[21,22,24,25] or perform amplification *in situ*.[23,26−29] Concentration factors up to

Received: April 15, 2016
Accepted: July 3, 2016

DOI: 10.1021/acs.analchem.6b01485
Anal. Chem. XXXX, XXX, XXX−XXX

15X[21,30] and limits-of-detection as sensitive as 10^4 copies/mL[23] or 500 cells/mL[26] have been reported. While these methods have clear advantages over traditional solid-phase extraction methods, processing time and lowest detectable concentration are still limited by their inability to handle large sample volumes (>1 mL)[26−28,31] and/or their slow processing rates, which range from μL/min to μL/h.[18,21,22,24,32,33] Thus, current methods—whether commercialized or from literature—lack the required combination of sensitivity, speed, and ease of implementation, leaving a gap in the current NA detection workflow.

We hypothesized that pressure-driven flow and capture in a porous matrix could facilitate the handling of large samples, while retaining many of the characteristics needed for both LRS and POC. Here, we analyze this approach theoretically and experimentally to determine a regime in which rapid, convection-driven capture is possible. Using a theoretical framework to predict capture efficiency as a function of flow-through conditions, we determined the parameters necessary for a detection matrix to capture a few nucleic acid molecules (<10 molecules) from several mLs of volume in short times (<10 min). We tested our predictions experimentally with respect to capture efficiency, lowest detectable concentration, processing time, and total sample volume. Furthermore, we demonstrated that the capture matrix is compatible with direct amplification, eliminating the need for an elution step. The ability to amplify *in situ* makes this approach amenable to integration into sample-to-answer devices and preserves the high concentration factors achieved during capture by preventing loss of target to the capture matrix during elution.

EXPERIMENTAL SECTION

Capture Simulations. The fraction of nucleic acid molecules captured in a membrane pore compared to the amount flowed through (capture efficiency) was simulated at steady-state using the *Transport of Diluted Species* module of *Comsol Multiphysics (version 4.4)*. A complete description of the model geometry, transport parameters, kinetics, boundary conditions, mesh, and calculations performed is included in the Supporting Information.

Chitosan Membrane Fabrication. A nylon membrane (LoProdyne LPNNG810S, Pall Corp., New York City, NY) was used as a porous matrix support. Two methods were employed for chitosan functionalization of the membrane, summarized below as "Method A" and "Method B".

Method A. The LoProdyne membrane has hydroxyl surface chemistry and was functionalized with *N*,*N*-carbonyldiimidazole (CDI) in methylene chloride according to the manufacturer's protocol (http://www.pall.com; Supporting Information S-VII).

Chitosan oligosaccharide lactate (No. 523682, Sigma-Aldrich, St. Louis, MO) was purified by dissolving 1.2 g of chitosan in 40 mL of nuclease-free (NF) water and then precipitated by adding 3 mL of 1 M NaOH. This solution was mixed and filtered through Whatman paper #8 (12 cm). It was then rinsed with Milli-Q water until the eluant was neutral. Washed chitosan was dried for 2 h under vacuum, and then a rotary evaporator was used to remove residual moisture.

The optimal pH at which to cross-link chitosan with CDI was determined to be pH 5.0. Based on the pK_a of chitosan (pK_a = 6.3), ∼5% of the chitosan's amines will be deprotonated and able to react. At pH > 5, a larger percentage of the chitosan amines will be deprotonated, resulting in a higher degree of cross-linking to the support surface and fewer available amines to interact with nucleic acids. At a pH of 5.0, the chitosan polymer should cross-link to the support at either one or two positions, leaving the bulk of the polymer free in solution.

To prepare chitosan-coated supports, a 6 mg/mL solution of purified chitosan was prepared in 34 mM HCl. This solution was vortexed for 10 min until the chitosan was fully dissolved and then sonicated to remove bubbles. The pH was then raised to 5.0 by addition of NaOH while vortexing. A CDI-functionalized LoProdyne membrane was then saturated with this chitosan solution. The membrane and chitosan solution were sandwiched between two glass slides and pressed to remove excess chitosan solution. The wet membrane was blot-dried and placed in a desiccator to dry under vacuum for 20−30 min. After drying, the membrane was placed in a 50 mL Falcon tube and rinsed with NF water. The water was poured out, 0.1 M HCl was added to quench any remaining CDI and remove non-cross-linked chitosan, and the membrane and HCl were vortexed for 2 min. The HCl was poured out, and the membrane was rinsed with NF water again. Next, the membrane was placed in a fresh Falcon tube, rinsed with NF water, washed in NF water for 25 min while agitated, rinsed with NF water three more times, blot dried, and then air-dried in a desiccator.

Method B. To prepare hydrogel coated membranes, a 0.5% (w/v) solution of chitosan (TCI OBR6I) was prepared in 150 mM HCl. A 25% (v/v) solution of glutaraldehyde was added to this solution to a final concentration of 4 mM. The solution was rapidly mixed and added to the LoProdyne membrane in excess. The saturated membranes were then spun on a Laurel WS-400-6NNP/Lite spin coater at 500 rpm for 5 s with an acceleration setting of 410, followed by 15 s at 2000 rpm with an acceleration setting of 820. Membranes were allowed to cross-link for 2 h in air, washed 3 times with NF water, and dried under vacuum.

Binding Capacity Measurements. 1000 ng of salmon sperm DNA (Invitrogen, Carlsbad CA) in 100 μL of 10 mM MES buffer (pH ∼ 5) was sequentially flushed through a chitosan membrane (radius = 2 mm, fabricated with Method A) five times via a syringe/luer lock system (Figure S-4). The inlet and eluate DNA concentration of each flush was measured with PicoGreen dye (Invitrogen); subtracting the eluate from the inlet and converting to mass of DNA yielded the plot in Figure 3.

Capture and *in Situ* Amplification. λ-Phage DNA stocks were quantified via digital PCR.[34] This DNA was spiked into varying volumes of 10 mM MES buffer (pH ∼ 5) to create concentrations ranging from 0.2 to 20 copies/mL (Table S-4). The solutions were flowed through chitosan-coated nylon membranes (radius = 2 mm) using syringes and luer locks (Figure S-4), followed twice by 100 μL of MES buffer. The membranes were then removed from the syringe/luer lock system and placed in an Ilumina Eco well plate, and 5−10 μL of PCR mix was added to each membrane. The well plate was inserted into an Ilumina Eco real time PCR system (EC-101-1001, Ilumina, San Diego, CA) and thermal cycled; correct λ-phage product was verified with a gel and melt curve analysis (Figure S-5).

The PCR mixture was used for amplification of λ-phage DNA on the chitosan-coated nylon membranes contained the following: 5 μL of 2X SsoFast Evagreen SuperMix (BioRad, Hercules, CA), 1 μL of BSA (20 mg/mL), 2 μL of 10 ng/uL salmon sperm DNA (Invitrogen), 1 μL of 5 μM primers (SI-

DOI: 10.1021/acs.analchem.6b01485
Anal. Chem. XXXX, XXX, XXX−XXX

VI), and 1 μL of NF water. The PCR amplification was performed with an initial 95 °C step for 3 min and then followed by 40 cycles of (i) 20 s at 95 °C, (ii) 20 s at 62 °C, and (iii) 15 s at 72 °C.

RESULTS AND DISCUSSION

Theoretical Analysis. To predict a regime that would enable rapid flow-through capture of nucleic acids present at low concentrations, we developed a theoretical model that takes into account the convection, diffusion, and adsorption of nucleic acid molecules onto a capture agent layered within a porous matrix (Figures 1a and S-I). Although the structure of

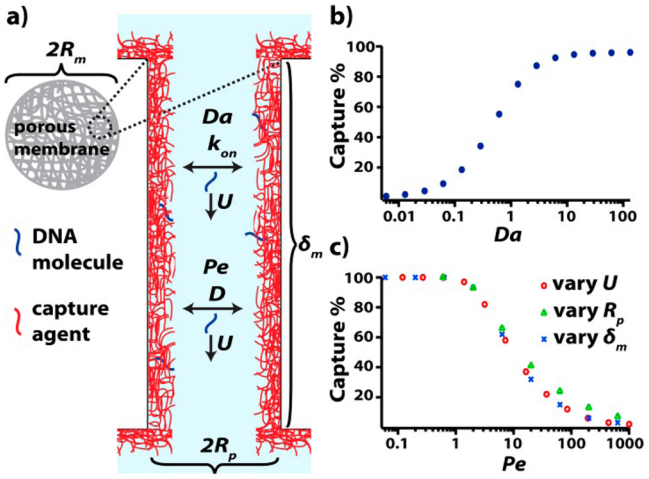

Figure 1. Theoretical model and numerical simulations for flow-through capture. a) A schematic drawing showing the process of capturing nucleic acids from a sample flowing through a porous membrane (which has been functionalized with a capture agent). b) Predictions for the percentage of molecules captured at the pore wall as a function of the Damköhler number (*Da*). c) Predictions for the percentage of molecules captured at the pore wall as a function of the Péclet number (*Pe*). *Pe* is changed by varying the velocity (U), pore length (δ_m), or pore radius (R_p); all result in a similar dependence of capture percentage on *Pe*.

the nylon membrane is spongy and nonuniform, approximating the pores as cylinders is an appropriate simplification to estimate the transport processes and has been done previously.[35,36] The parameters governing capture dynamics in a cylindrical pore are superficial velocity U [m/s], pore radius R_p [m], membrane radius R_m [m], membrane thickness (or, equivalently, pore length) δ_m [m], diffusivity of nucleic acid molecules[37] D [m^2/s], association rate constant[38] k_{on} [m^3/(mol·s)], surface concentration of the capture agent γ [mol/m^2], and mass transfer coefficient k_c [m/s]. Instead of analyzing every relevant parameter individually, we condensed them into two dimensionless numbers:[39,40] Damköhler (*Da*) and Péclet (*Pe*). *Da* characterizes the balance between adsorption rate and transport rate (eq 1), while *Pe* characterizes the balance between convection rate and diffusion rate (eq 2).

$$Da = \frac{\text{adsorption rate}}{\text{transport rate}} = \frac{k_{on}\gamma}{k_c}, \quad k_c = 1.62\left(\frac{UD^2}{2\delta_m R_p}\right)^{1/3} \tag{1}$$

$$Pe = \frac{\text{convection rate}}{\text{diffusion rate}} = \frac{U/\delta_m}{D/R_p^2} \tag{2}$$

Da > 1 indicates that the rate of DNA binding to the capture agent is faster than the rate of DNA transport to the pore wall; *Pe* < 1 means the rate at which molecules diffuse to the pore wall is faster than the rate at which they are convected through the pore. To capture dilute nucleic acids from large volumes in short times, two conditions must be met: (i) efficient capture (*Da* ≫ 1) and (ii) fast flow rates (∼ 1 mL/min) while maintaining *Pe* < 1.

Capture efficiency is a factor of binding kinetics (time for the nucleic acid molecule to bind to the capture agent) and transport (time for the nucleic acid molecule to travel from the bulk solution to the pore wall coated with capture agent). High capture efficiency occurs when the transport rate is slower than the binding reaction rate (i.e., *Da* ≫ 1), which can occur with fast reactions or slow transport. Many passive capture processes—such as wicking through a porous matrix or mixing with beads—rely on slow transport rates to achieve high *Da*. These processes capture efficiently at small length scales in microliter volumes;[21−23,33] however, for milliliter volumes and large length scales, passive capture processes would require impractical amounts of capture agent or time for *Da* to be greater than 1. A fast binding reaction with diffusion-limited kinetics would enable higher transport rates (and thus faster flow rates) without adversely affecting capture efficiency. Electrostatic binding and silica adsorption in the presence of Ca^{2+} are examples of diffusion-limited chemical reactions[41,42] that would maintain high *Da* without relying on slow transport rates to ensure efficient capture. Our simulations show that when a capture agent coated on a pore wall has fast binding kinetics, *Da* > 10 ensures >95% capture of nucleic acids flowing through the pore (Figure 1b and S-I). To scale up efficient capture processes to larger volumes, the mass transport rate can be increased. One way to increase mass transport rate is actively forcing fluid through a porous matrix,[43] which has been used for protein capture[44] and is well established in membrane chromatography.[35,36] However, flow-through capture has not been analyzed theoretically nor tested experimentally for rapid capture and detection of zeptomolar nucleic acids.

In general, high flow rates increase the transport rate, decrease *Da*, and thus reduce capture efficiency. However, the transport rate can be maintained below the adsorption rate (keeping *Da* ≫ 1) by manipulating other transport parameters, thus counteracting the high flow rate. These transport parameters can be analyzed together by simulating the capture efficiency as a function of *Pe* (S-I): simulations show that keeping *Pe* < 1 ensures >90% capture efficiency (Figure 1c). To achieve a high convection rate and maintain *Pe* < 1, a relatively high diffusion rate is required, which ensures that the molecules do not leave the pore before having a chance to diffuse to the wall and bind. To maintain this balance of a high convection rate with an even higher diffusion rate, the membrane radius, pore radius, and membrane thickness can be adjusted. Setting *Pe* < 1 in eq 2 provides the following constraint on flow rate through the membrane (Q) as a function of δ_m, R_m, and R_p, where ϕ represents the porosity of the membrane (see S-II for derivation).

$$Q < \frac{\pi\phi D\delta_m R_m^2}{R_p^2} \tag{3}$$

DOI: 10.1021/acs.analchem.6b01485
Anal. Chem. XXXX, XXX, XXX−XXX

Plotting eq 3 at different membrane thicknesses explores the relationship of these parameters (Figure 2a); trends favoring *Pe* < 1 and flow rates >1 mL/min are decreasing pore radius, increasing membrane radius, and increasing membrane thickness. Decreasing the pore size enables faster diffusion rates and lower *Pe*, but it also increases the resistance to flow. Figure 2b considers this trade-off, showing the pressure drop (ΔP) required for a sample to flow through the membrane at 1 mL/min at different membrane and pore radii. The overlap of the green triangles (*Pe* < 1) with red color (ΔP < 1 atm) represents an ideal combination of parameters wherein *Pe* is low enough and a reasonable pressure drop is achieved to flow at 1 mL/min.

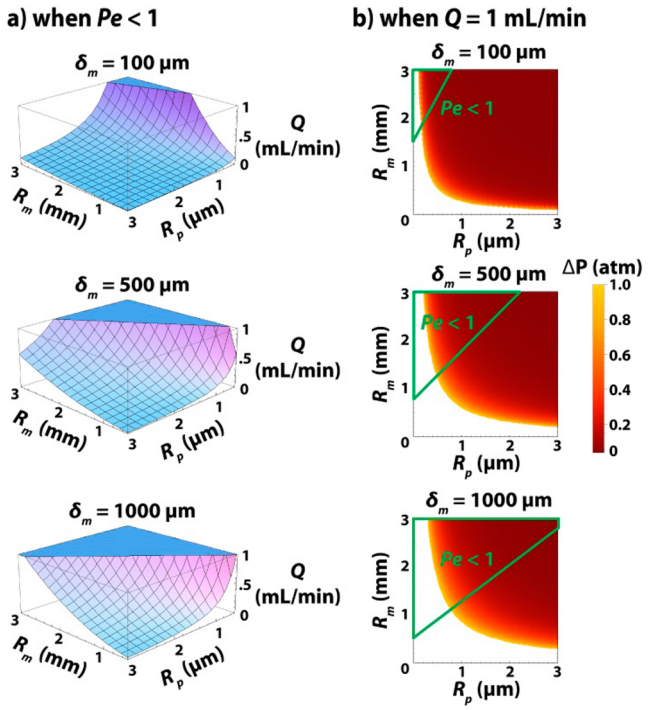

Figure 2. Predictions of membrane radius, pore radius, and membrane thickness trade-offs for achieving high flow rates while also maintaining reasonable pressure drop (ΔP) and a low Péclet number (*Pe*). a) Combinations of membrane radius, pore radius, and flow rate that maintain *Pe* < 1 for different membrane thicknesses. Any point below the surface curvature has *Pe* < 1. b) The influence of membrane and pore radius on pressure drop with the flow rate through the membrane held constant at 1 mL/min. The overlap of the green triangle (*Pe* < 1) and red colored area represents efficient and rapid capture with a reasonable pressure drop (ΔP < 1 atm). The white area signifies a combination of membrane and pore radius that results in prohibitively large pressure drops (ΔP > 1 atm) necessary to achieve 1 mL/min.

Experimental Analysis. Based on these predictions, we chose an appropriate experimental system to evaluate the ability of a flow-through matrix to rapidly capture zeptomolar concentrations of nucleic acids. This matrix should be compatible with *in situ* amplification, so glass fiber, silica, and other common capture materials that inhibit amplification reactions were not considered.[45,46] Nylon membranes do not prevent nucleic acid amplification and can be purchased in various pore sizes and thicknesses. The membrane thickness for a LoProdyne nylon membrane from Pall Corporation ranges from 127.0 to 190.5 μm (see the Experimental Section); at this thickness, a membrane radius of 2 mm is flexible and easily placed in a well plate for nucleic acid amplification. For a membrane thickness of 160 μm, flow rate of 1 mL/min, and membrane radius of 2 mm, eq 3 predicts that pore radii less than 0.76 μm would maintain *Pe* < 1. Therefore, we chose LoProdyne membranes with a pore radius of 0.6 μm; coating the membrane pores with a capture agent makes the pore size even smaller, ensuring that we were well below the 0.76 μm requirement. As described, the capture agent must have diffusion-limited kinetics. Because electrostatic binding is very fast and can easily be used for nucleic acid capture by utilizing a cationic polymer to attract the negatively charged phosphate backbone of DNA, we chose chitosan as the capture agent, which has previously been used for NA capture.[21−25] Chitosan is an inexpensive biocompatible polymer with amine groups on its backbone that become positively charged when the pH is below 6.3.[22,47] We functionalized chitosan onto the nylon membrane as described in the Experimental Section. To verify that functionalizing the membrane with chitosan does not reduce the pore size such that the pressure drop becomes untenable (Figure 2b), we measured the capture efficiency at different flow rates. This experiment showed that the chitosan-functionalized nylon membrane captures >90% of nucleic acids when solution is flowed through at 1 mL/min (see Figure S-2 of the Supporting Information).

To test the predictions from our analysis, we evaluated the capture efficiency as a function of *Pe* by flowing 500 ng/mL solutions of DNA through chitosan-functionalized nylon membranes at five different flow rates. Each flow rate was tested with three replicates, and the capture efficiency along with one standard deviation is plotted in Figure S-2. These experiments confirmed that the chitosan membranes capture efficiently over a range of *Pe*, with >90% capture of DNA when *Pe* < 1 (Figure S-2). We also measured the DNA binding capacity of chitosan-functionalized nylon membranes and found that they have a capacity of 1000 ng or more (Figure 3). This capacity is much greater than needed for our target application of zeptomolar concentrations (10^{-21} M ∼ 0.6 fg/mL for a bacterial genome). However, researchers in other fields may find this matrix useful in capturing large amounts of genetic material for other applications.

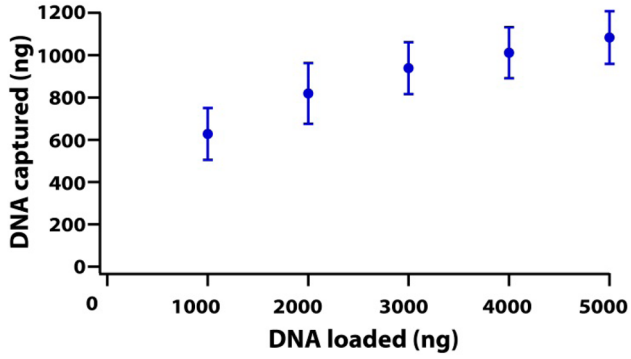

Figure 3. DNA binding capacity of chitosan-functionalized membranes fabricated with Method A. Error bars are SD.

Next, we tested whether *in situ* amplification would be chemically compatible with a nylon membrane functionalized with chitosan. We added serial dilutions of DNA to the membrane and then submerged it in amplification mix and amplified the DNA via PCR. The chitosan membrane was compatible with *in situ* PCR amplification down to ∼2 copies

DOI: 10.1021/acs.analchem.6b01485
Anal. Chem. XXXX, XXX, XXX−XXX

per reaction (Figure S-3a). We also tested the chitosan membrane compatibility with *in situ* LAMP and showed successful amplification at 20 copies per reaction (Figure S-3b[48]).

In this paper we did not study the location at which amplification occurs (i.e., whether amplification is initiated on the target molecules still attached to the surface of the membrane, or on the molecules released from the surface into the membrane pores, or on the molecules diffusing out of the pores). Further, we did not study the spatiotemporal mechanism of propagation of amplification once it is initiated. Such studies could provide interesting information in subsequent research.

The final step was to use chitosan's charge-switch capability to couple rapid capture with direct amplification without eluting the nucleic acids. A sample flows through the chitosan-coated membrane at pH ~ 5, and the negatively charged phosphate backbone of DNA will electrostatically bind to the positively charged amine groups on the chitosan. Following capture of NAs, the addition of amplification mix at pH ~ 8 deprotonates the amine groups and releases the captured nucleic acids for amplification (Figure 4).

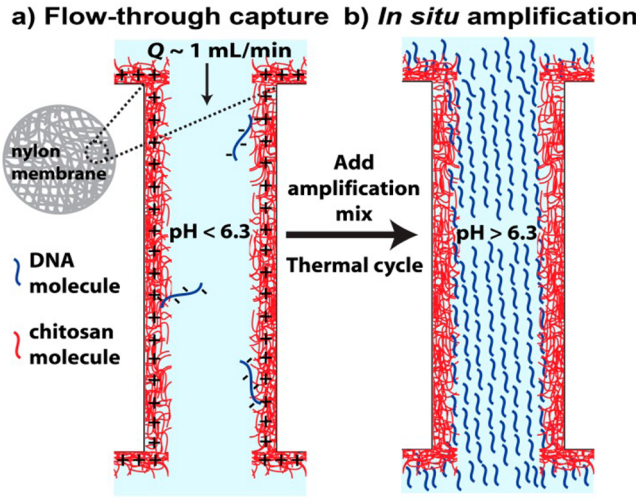

Figure 4. Schematic of capture and *in situ* amplification. a) Nucleic acids in a solution with pH < 6.3 will electrostatically bind to the protonated chitosan pore wall. b) Addition of amplification mix (pH ~ 8) deprotonates the chitosan and releases nucleic acids, which are then amplified *in situ*.

We then tested this idea (combining rapid capture and *in situ* amplification via charge-switch) at ultralow concentrations (~1 copy/mL) and fast flow rates. Various amounts of λ DNA were spiked into volumes ranging from 1 to 50 mL with 100 ng or less background DNA (Table S-4); the solution was then flowed through a 2 mm radius chitosan-functionalized membrane at ~1 mL/min. After capture, the amplification was performed *in situ* with small volumes of PCR reagents (5–10 μL), as opposed to the traditional method of eluting from a capture matrix and using larger volumes of PCR reagents. DNA product was detected after thermal cycling using EvaGreen dye (see SI-V for details). This methodology detected a DNA target at concentrations as low as 0.5 copies/mL from as many as 50 mL (Figure 5b). Compiling data from replicate experiments run on different days, preconcentration using the chitosan-functionalized membrane allowed detection down to 1 copy/

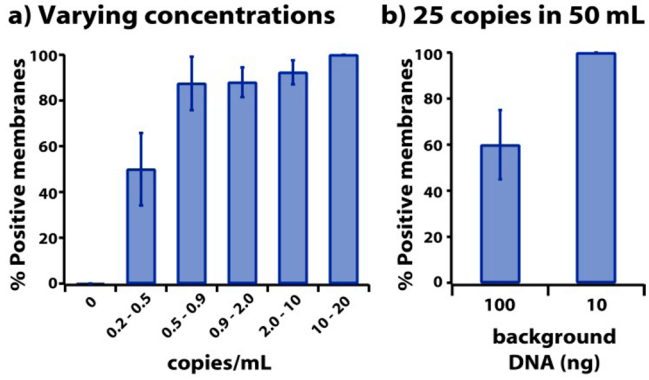

Figure 5. Nucleic acid detection via flow-through capture and *in situ* amplification on chitosan-functionalized nylon membranes. a) Percent of membranes that were positive for λ DNA product over different experiments on different days for varying concentrations (0.2–20 copies/mL). The volume flowed through the membrane ranged from 1 to 50 mL (Table S-4), and the flow rate was ~1 mL/min. Each bin of the histogram has 6–26 samples for a total of 82 samples. b) Percent of membranes that were positive for λ DNA product over different experiments on different days. 50 mL solutions with 25 copies of target DNA and 10 or 100 ng background DNA were flowed through membranes at ~0.3 mL/min. N = 10 for 100 ng and N = 9 for 10 ng. All error bars are 1 SD.

mL over 85% of the time. Using any concentration above 10 copies/mL, detection results for the capture and amplification matrix were positive 100% of the time. No amplification was detected when flowing through buffer without DNA (see Figure 5a and Table S-4), ensuring that the λ DNA product detected is indeed from the sample flowed through the membrane and not contamination of the membrane, lab materials, or PCR reagents with λ-phage DNA.

We observed that the chitosan membrane performance appeared to decrease slightly as larger volumes were flowed through it (e.g., >10 mL volumes were 77% positive (23 out of 30 tests) and >20 mL volumes were 60% positive (9 out of 15 tests), see Table S-4). This decreased performance at higher volumes could be due to chitosan being shed from the membrane during flow or the fact that larger volumes have longer residence times and therefore more opportunity for a DNA molecule to release from its binding site and be flushed out of the membrane with the eluate. A thicker membrane with longer pores or a chitosan-functionalization method that more strongly attaches chitosan to the nylon membrane could potentially improve its performance at larger volumes; however, these parameters were not tested and are outside of the scope of this study.

Our experiments used stringent conditions with high flow rate (~1 mL/min) and high level of added background DNA. For some applications, these conditions might be too stringent, and high sensitivity of detection may be more valuable. For example, drinking water samples do not always have the high level of background DNA we used. The presence of high levels of background DNA can affect capture efficiency of the target molecule during flow-through and can affect amplification efficiency during PCR. We therefore also tested detection of ultralow concentrations of nucleic acids from large volumes with reduced background DNA at 10 ng and slower flow rates at 0.3 mL/min. We compared 50 mL solutions with 100 ng of background DNA to 50 mL solutions with 10 ng of background DNA. These experiments showed that 25 copies in 50 mL

DOI: 10.1021/acs.analchem.6b01485
Anal. Chem. XXXX, XXX, XXX–XXX

could be consistently detected under these conditions (Figure 5b). We have not yet further investigated how the performance of this method depends on the interplay of flow rate, pore geometry, concentration of background DNA, and the details of fabrication of the chitosan coating. To test whether salts in solution could interfere with electrostatic binding and decrease the ability of chitosan membranes to capture and detect nucleic acids, we performed six preliminary experiments. The experiments were identical to those performed for Figure 5a, but instead of using 10 mM MES buffer as the medium comprising nucleic acids, the following salt solutions were used (see S-VIII for details): (i) Ringer's solution (10 and 20 copies λ DNA in 1 mL), Ringer's solution with 5 mM EDTA (10 and 20 copies λ DNA in 1 mL), and 5 mM EDTA alone (10 and 20 copies λ DNA in 1 mL). All six experiments resulted in positive amplification, indicating that the presence of salts does not disrupt capture of nucleic acids on the chitosan-functionalized nylon membrane nor their subsequent amplification.

CONCLUSION

We evaluated an approach for ultrasensitive detection of nucleic acids using chitosan as a charge-switch matrix that enables concentration factors up to 5000X (defined as the ratio of final detection volume to the starting sample volume, e.g., DNA from 50 mL of solution was detected in 10 μL of PCR mix) and subsequent *in situ* amplification. A theoretical model guided the parameters chosen for flow rate, membrane radius, and pore radius. Based on model predictions, membranes with specific pore and membrane radii were functionalized to capture low copy numbers of nucleic acids from large volumes in short times. Using this approach, we were able to capture zeptomolar concentrations of nucleic acids from up to 50 mL of solution at a flow rate of 1 mL/min with $\Delta P < 1$ atm. In applications with different requirements for flow rate, pressure drop, or membrane size, this theory can be applied to guide choices of membrane parameters that meet those requirements.

In addition, flowing through a matrix that is compatible with *in situ* amplification obviates the need for centrifugation or bead manipulation and simplifies the purification process by eliminating an elution step. Chitosan-functionalized nylon membranes are sturdy, flexible, and small enough to be incorporated into integrated devices for complete sample-to-answer diagnostics. In this study, we focused on the theory and the proof-of-principle experiments using solutions of purified nucleic acids in clean matrixes. However, more complex matrices are encountered in many applications. Ultrasensitive measurements of viral, bacterial, and cancer-associated nucleic acids provide important diagnostic information to clinicians but require the extraction and detection of NAs from milliliters of plasma and in some cases cell lysis. Combining this approach with lysis buffers and/or sample pretreatment should be tested next to evaluate the efficacy of this methodology for detection from a variety of sample matrices, such as blood, plasma, urine, and water. Additional work to integrate this approach with isothermal amplification would enable rapid and ultrasensitive nucleic acid measurements for point-of-care and limited-resource settings.

ASSOCIATED CONTENT

Supporting Information

The Supporting Information is available free of charge on the ACS Publications website at DOI: 10.1021/acs.analchem.6b01485.

Additional materials, methods, and supporting Figures S1−S5 (PDF)

AUTHOR INFORMATION

Corresponding Author

*Fax: (626) 568-8743. E-mail: rustem.admin@caltech.edu.

Present Address

†Chemical & Biological Engineering Department, Montana State University, 306 Cobleigh Hall, P.O. Box 173920, Bozeman, MT 59717 USA.

Author Contributions

‡T.S.S. and S.E.M. contributed equally. T.S.S., S.E.M., N.G.S., and R.F.I. designed the study and wrote the manuscript. T.S.S. and S.E.M. performed theoretical analysis. T.S.S., S.E.M., and N.G.S. performed experiments and data analysis.

Notes

The authors declare no competing financial interest.

ACKNOWLEDGMENTS

This work was supported by DARPA Cooperative Agreement HR0011-11-2-0006. The content of this article does not necessarily reflect the position or the policy of the Government, and no official endorsement should be inferred. We thank Justin Rolando for chemistry advice and chitosan purification and Natasha Shelby for contributions to writing and editing this manuscript.

REFERENCES

(1) Fearon, M.; Scalia, V.; Lane, D.; Bigham, M.; Hawes, G.; O'Brien, S.; Kadkhoda, K. *Transfusion* **2016**, *56*, 994−995.

(2) Fong, T.-T.; Lipp, E. K. *Microbiol. Mol. Biol. Rev.* **2005**, *69*, 357−371.

(3) Hodgson, S. H.; Douglas, A. D.; Edwards, N. J.; Kimani, D.; Elias, S. C.; Chang, M.; Daza, G.; Seilie, A. M.; Magiri, C.; Muia, A. *Malar. J.* **2015**, *14*, 33.

(4) World Health Organization. *Guidelines for Drinking-water Quality: Recommendations*, 3rd ed.; World Health Organization: Geneva, 2004; Vol. *1*.

(5) Raboud, J. M.; Montaner, J. S.; Conway, B.; Rae, S.; Reiss, P.; Vella, S.; Cooper, D.; Lange, J.; Harris, M.; Wainberg, M. A. *AIDS* **1998**, *12*, 1619−1624.

(6) Sarmati, L.; D'Ettorre, G.; Parisi, S. G.; Andreoni, M. *Curr. HIV Res.* **2015**, *13*, 250.

(7) Jiang, S.; Noble, R.; Chu, W. *Appl. Environ. Microbiol.* **2001**, *67*, 179−184.

(8) Haramoto, E.; Kitajima, M.; Katayama, H.; Ohgaki, S. *Water Res.* **2010**, *44*, 1747−1752.

(9) Campana, D.; Pui, C.-H. *Blood* **1995**, *85*, 1416−1434.

(10) Maggiolo, F.; Callegaro, A.; Cologni, G.; Bernardini, C.; Velenti, D.; Gregis, G.; Quinzan, G.; Soavi, L.; Iannotti, N.; Malfatto, E. *JAIDS, J. Acquired Immune Defic. Syndr.* **2012**, *60*, 473−482.

(11) Castillo, I.; Bartolome, J.; Quiroga, J.; Barril, G.; Carreño, V. *Aliment. Pharmacol. Ther.* **2009**, *30*, 477−486.

(12) Keys, J. R.; Leone, P. A.; Eron, J. J.; Alexander, K.; Brinson, M.; Swanstrom, R. *J. Med. Virol.* **2014**, *86*, 473−477.

(13) Abubakar, A.; Ozumba, P.; Buttner, P.; Winter, J.; Abimiku, A. *Journal of Antivirals & Antiretrovirals* **2015**, *2015*, 7:89-103.

(14) Yager, P.; Domingo, G. J.; Gerdes, J. *Annu. Rev. Biomed. Eng.* **2008**, *10*, 107−144.

(15) Urdea, M.; Penny, L. A.; Olmsted, S. S.; Giovanni, M. Y.; Kaspar, P.; Shepherd, A.; Wilson, P.; Dahl, C. A.; Buchsbaum, S.; Moeller, G. *Nature* **2006**, *444*, 73−79.

(16) Boom, R.; Sol, C.; Salimans, M.; Jansen, C.; Wertheim-van Dillen, P.; Van der Noordaa, J. *J. Clin. Microbiol.* **1990**, *28*, 495−503.

DOI: 10.1021/acs.analchem.6b01485
Anal. Chem. XXXX, XXX, XXX−XXX

(17) Wen, J.; Legendre, L. A.; Bienvenue, J. M.; Landers, J. P. *Anal. Chem.* **2008**, *80*, 6472−6479.
(18) Dineva, M. A.; Mahilum-Tapay, L.; Lee, H. *Analyst* **2007**, *132*, 1193−1199.
(19) Chomczynski, P.; Sacchi, N. *Anal. Biochem.* **1987**, *162*, 156−159.
(20) Miller, D.; Bryant, J.; Madsen, E.; Ghiorse, W. *Appl. Environ. Microbiol.* **1999**, *65*, 4715−4724.
(21) Byrnes, S. A.; Bishop, J. D.; Lafleur, L.; Buser, J.; Lutz, B.; Yager, P. *Lab Chip* **2015**, *15*, 2647−2659.
(22) Cao, W.; Easley, C. J.; Ferrance, J. P.; Landers, J. P. *Anal. Chem.* **2006**, *78*, 7222−7228.
(23) Pandit, K. R.; Nanayakkara, I. A.; Cao, W.; Raghavan, S. R.; White, I. M. *Anal. Chem.* **2015**, *87*, 11022−11029.
(24) Hagan, K. A.; Meier, W. L.; Ferrance, J. P.; Landers, J. P. *Anal. Chem.* **2009**, *81*, 5249−5256.
(25) Kendall, E. L.; Wienhold, E.; DeVoe, D. L. *Biomicrofluidics* **2014**, *8*, 044109.
(26) Connelly, J. T.; Rolland, J. P.; Whitesides, G. M. *Anal. Chem.* **2015**, *87*, 7595−7601.
(27) Rodriguez, N. M.; Linnes, J. C.; Fan, A.; Ellenson, C. K.; Pollock, N. R.; Klapperich, C. M. *Anal. Chem.* **2015**, *87*, 7872−7879.
(28) Liu, C.; Geva, E.; Mauk, M.; Qiu, X.; Abrams, W. R.; Malamud, D.; Curtis, K.; Owen, S. M.; Bau, H. H. *Analyst* **2011**, *136*, 2069−2076.
(29) Rodriguez, N. M.; Wong, W. S.; Liu, L.; Dewar, R.; Klapperich, C. M. *Lab Chip* **2016**, *16*, 753−763.
(30) Reedy, C. R.; Bienvenue, J. M.; Coletta, L.; Strachan, B. C.; Bhatri, N.; Greenspoon, S.; Landers, J. P. *Forensic Sci. Int.: Genet.* **2010**, *4*, 206−212.
(31) Jangam, S. R.; Yamada, D. H.; McFall, S. M.; Kelso, D. M. *J. Clin. Microbiol.* **2009**, *47*, 2363−2368.
(32) Breadmore, M. C.; Wolfe, K. A.; Arcibal, I. G.; Leung, W. K.; Dickson, D.; Giordano, B. C.; Power, M. E.; Ferrance, J. P.; Feldman, S. H.; Norris, P. M. *Anal. Chem.* **2003**, *75*, 1880−1886.
(33) Shim, S.; Shim, J.; Taylor, W. R.; Kosari, F.; Vasmatzis, G.; Ahlquist, D. A.; Bashir, R. *Biomed. Microdevices* **2016**, *18*, 1−8.
(34) Shen, F.; Du, W.; Kreutz, J. E.; Fok, A.; Ismagilov, R. F. *Lab Chip* **2010**, *10*, 2666−2672.
(35) Thömmes, J.; Kula, M. R. *Biotechnol. Prog.* **1995**, *11*, 357−367.
(36) Unarska, M.; Davies, P.; Esnouf, M.; Bellhouse, B. *J. Chromatogr. A* **1990**, *519*, 53−67.
(37) Lukacs, G. L.; Haggie, P.; Seksek, O.; Lechardeur, D.; Freedman, N.; Verkman, A. *J. Biol. Chem.* **2000**, *275*, 1625−1629.
(38) Wink, T.; de Beer, J.; Hennink, W. E.; Bult, A.; van Bennekom, W. P. *Anal. Chem.* **1999**, *71*, 801−805.
(39) Hansen, R.; Bruus, H.; Callisen, T. H.; Hassager, O. *Langmuir* **2012**, *28*, 7557−7563.
(40) Koyayashi, T.; Laidler, K. J. *Biotechnol. Bioeng.* **1974**, *16*, 99−118.
(41) Nguyen, T. H.; Elimelech, M. *Biomacromolecules* **2007**, *8*, 24−32.
(42) Minehan, D. S.; Marx, K. A.; Tripathy, S. K. *Macromolecules* **1994**, *27*, 777−783.
(43) Chung, Y.-C.; Jan, M.-S.; Lin, Y.-C.; Lin, J.-H.; Cheng, W.-C.; Fan, C.-Y. *Lab Chip* **2004**, *4*, 141−147.
(44) Bhattacharjee, S.; Dong, J.; Ma, Y.; Hovde, S.; Geiger, J. H.; Baker, G. L.; Bruening, M. L. *Langmuir* **2012**, *28*, 6885−6892.
(45) Wang, W.; Wang, H. B.; Li, Z. X.; Guo, Z. Y. *J. Biomed. Mater. Res., Part A* **2006**, *77A*, 28−34.
(46) Linnes, J.; Rodriguez, N.; Liu, L.; Klapperich, C. *Biomed. Microdevices* **2016**, *18*, 1−12.
(47) Kyung-Hee, C.; Kwang-hee, K. P. *Bull. Korean Chem. Soc.* **1983**, *4*, 68−72.
(48) Nagamine, K.; Hase, T.; Notomi, T. *Mol. Cell. Probes* **2002**, *16*, 223−229.

DOI: 10.1021/acs.analchem.6b01485
Anal. Chem. XXXX, XXX, XXX−XXX